

Geophysical Research Letters

RESEARCH LETTER

10.1029/2019GL085504

Key Points:

- Single foraminiferal Mg/Ca data show lower El Niño amplitude in the early Pliocene than the late Holocene
- By ~3.1 Ma, El Niño amplitude was sometimes lower than and sometimes similar to the late Holocene, varying on millennial timescales
- Our data verify models showing weaker El Niño when vertical and zonal temperature gradients are lower, due to weaker thermocline feedback

Supporting Information:

- Supporting Information S1

Correspondence to:

S. M. White,
 smwhite@ucsc.edu

Citation:

White, S. M., & Ravelo, A. C. (2020). Dampened El Niño in the early Pliocene warm period. *Geophysical Research Letters*, 47, e2019GL085504. <https://doi.org/10.1029/2019GL085504>

Received 22 SEP 2019

Accepted 28 JAN 2020

Accepted article online 30 JAN 2020

Dampened El Niño in the Early Pliocene Warm Period

S. M. White¹  and A. C. Ravelo² 

¹Department of Earth and Planetary Sciences, University of California, Santa Cruz, CA, USA, ²Department of Ocean Sciences, University of California, Santa Cruz, CA, USA

Abstract El Niño-Southern Oscillation (ENSO) is the strongest mode of interannual climate variability, and its predicted response to anthropogenic climate change remains unclear. Determining ENSO's sensitivity to climatic mean state and the strength of positive and negative feedbacks, notably the thermocline feedback, will help constrain its future behavior. To this end, we collected ENSO proxy data from the early and mid-Pliocene, a time during which tropical Pacific zonal and vertical temperature gradients were much lower than today. We found that El Niño events had a reduced amplitude throughout the early Pliocene, compared to the late Holocene. By the mid-Pliocene, El Niño amplitude was variable, sometimes reduced and sometimes similar to the late Holocene. This trend in Pliocene ENSO amplitude mirrors the long-term strengthening of zonal and vertical temperature gradients and verifies model results showing dampened ENSO under reduced gradients due to a weaker thermocline feedback.

Plain Language Summary El Niño events are marked by anomalously warm sea-surface temperatures and increased rainfall in the central and eastern equatorial Pacific and cause major changes in weather patterns across the Pacific. It is unclear whether El Niño events will strengthen or weaken with anthropogenic warming. To help elucidate El Niño's future behavior, we reconstructed changes in El Niño during the Pliocene, the most recent extended period that was warmer than today. We found that El Niño events were weaker ~3.5 to 5 Ma, compared to the late Holocene. By ~3.1 Ma, El Niño strength was sometimes weaker and sometimes similar to the late Holocene, varying on millennial timescales. The shift in El Niño behavior coincides with a long-term cooling of tropical Pacific subsurface waters. The association between subsurface temperature and El Niño strength has also been observed for the Last Glacial Maximum and the Holocene and points to an important role of the subsurface in dictating El Niño strength.

1. Introduction

El Niño events, marked by anomalously warm sea-surface temperatures (SSTs) in the eastern and central equatorial Pacific, cause drought, floods, and ecosystem shifts over the circum-Pacific region and occur every 3 to 7 years as part of El Niño-Southern Oscillation (ENSO). ENSO is the strongest mode of interannual climate variability, and its predicted response to anthropogenic climate change remains unclear. The disparity among predictions stems from a lack of understanding of ENSO's sensitivity to changes in mean climate and positive and negative feedbacks, including the thermocline and upwelling feedbacks. Paleoproxy data from the Holocene and Last Glacial Maximum indicate that tropical Pacific thermocline depth, a major control on the strength of the thermocline and upwelling feedbacks, seems to dictate the strength of El Niño events (Ford, Ravelo, & Polissar, 2015; White et al., 2018). However, different models place different emphasis on these feedbacks, which creates disparity in simulations of modern ENSO (Kim et al., 2014), and different models exhibit differing changes in strength of the thermocline feedback under future warming (Chen et al., 2017).

The Pliocene is an excellent test case of the importance of thermocline depth, because the tropical Pacific thermocline was much deeper than today in the early Pliocene and shoaled toward present [Ford et al., 2012; Ford, Ravelo, Dekens, et al., 2015; Seki et al., 2012; Steph et al., 2010]. The eastern equatorial Pacific (EEP) was also much warmer (Dekens et al., 2007; Lawrence et al., 2006; Rousselle et al., 2013; Zhang et al., 2014), resulting in a state referred to as “El Padre,” to highlight that the reduced zonal temperature gradient and deeper thermocline describe long-term mean state (Ford, Ravelo, Dekens, et al., 2015). ENSO is expected to have existed in the El Padre state but may have been dampened (Burls & Fedorov, 2014; Manucharyan & Fedorov, 2014). Modeling efforts, including the PlioMIP model intercomparison, focus on the mid-Pliocene PRISM interval (Pliocene Research, Interpretation and Synoptic Mapping,

3.264–3.025 Ma). However, the warmest surface and subsurface temperatures occurred before ~4 Ma, in the early Pliocene. Other studies tested effects of various factors during the early Pliocene, including an open Central American Seaway (CAS), a deeper/wider Indonesian seaway, higher $p\text{CO}_2$, weaker zonal winds and SST gradients, altered Andean orography, and a deeper thermocline (Brierley & Fedorov, 2016; Burls & Fedorov, 2014; Feng & Poulsen, 2014; Jochum et al., 2009; Manucharyan & Fedorov, 2014; Song et al., 2017; von der Heydt et al., 2011), but report different effects on ENSO depending on the model and boundary conditions. Centennial-scale variability in ENSO adds further difficulty, necessitating longer model runs and larger proxy data sets to achieve confidence in interpreting results (e.g., Tindall et al., 2016). Although there are limited ENSO data from the mid-Pliocene (Scroxton et al., 2011; Watanabe et al., 2011), none are from the early Pliocene.

New data from the early Pliocene are thus needed to test ENSO's response to a deeper thermocline and lower east-west temperature gradient. Manucharyan and Fedorov (2014) found that ENSO was dampened under these conditions due to a weaker thermocline feedback, in a general circulation model whose physics were altered to produce lower zonal and vertical temperature gradients in the tropical Pacific, but no proxy data exist to verify this result. To this end, we collected individual foraminiferal temperature data from the EEP. We analyzed samples every half million years from 5 Ma to the PRISM interval, plus multiple samples at high resolution in the PRISM interval and 4.5 Ma, to evaluate long-term trends in ENSO strength and verify the presence/absence of shorter timescale variations.

This study focuses on ODP Site 849 in the EEP, located within the Niño3 region (Figure 1). The site is well suited for studying ENSO; the seasonal range of SST is $\pm 1.5^\circ\text{C}$, whereas the average peak El Niño anomaly is $+2.8^\circ\text{C}$, and the very warmest temperatures occur exclusively during El Niño months, as shown in a reanalysis data set (Simple Ocean Data Assimilation; Carton & Giese, 2008). We are thus able to distinguish changes in seasonality versus ENSO, as described below.

2. Methods

2.1. Analytical Methods

To reconstruct El Niño strength at Site 849, we collected foraminiferal Mg/Ca ratios from individual tests of the mixed-layer dwelling foraminifer *Globigerinoides sacculifer* without sac-like chamber, that is, *Trilobatus trilobus* (Spezzaferri et al., 2015); here we retain the name *G. sacculifer* for consistency with White et al. (2018). Mg/Ca data were acquired by LA-ICP-MS following White et al. (2018) on an average of 48 specimens per sample (supporting information Table S1).

2.2. Temperature Calibration and Age Estimates

We converted foraminiferal Mg/Ca ratios to temperature using a species-specific calibration with depth-based dissolution correction (Dekens et al., 2002). Sample ages are from the Mix et al. (1995) age model, which is based on benthic foraminiferal $\delta^{18}\text{O}$ data from our site. The time represented in each sample varies from ~1,250–1,600 years in the early Pliocene to ~2,900 years in the mid-Pliocene, based on sedimentation rate and an estimated bioturbation depth of 8 cm (Trauth et al., 1997). The longer time span of Pliocene samples versus the late Holocene comparison sample (which spans ~600 years; Ford, Ravelo, & Polissar, 2015) means that the Pliocene samples may include more centennial variations in mean temperature, which may increase observed temperature variability. Samples dated to 3.071, 3.082, and 3.087 Ma are from Hole 849C, whereas all others are from Hole 849D. As such, there is some uncertainty (a few thousand years) in the ages of these samples relative to all others, so samples may be further apart in age than they appear. We note that in an individual foraminiferal data set, bioturbation does not reduce variance but rather broadens the time frame over which temperatures are sampled.

2.3. Reconstruction of Temperature Variability and El Niño Strength

Because *G. sacculifer* lives for about 1 month (Bijma et al., 1990), acquiring data from many individuals provides a reconstruction of the monthly temperature distribution. To diagnose changes in Pliocene ENSO, we use quantile-quantile (QQ) plots, a method that compares distributions enabling visual separation of El Niño from seasonality. Pliocene samples are normalized to the late Holocene sample to minimize bias from bioturbation and other sedimentary or foraminiferal processes and remove changes in mean temperature. The 95% confidence intervals are estimated by Monte Carlo bootstrapping of

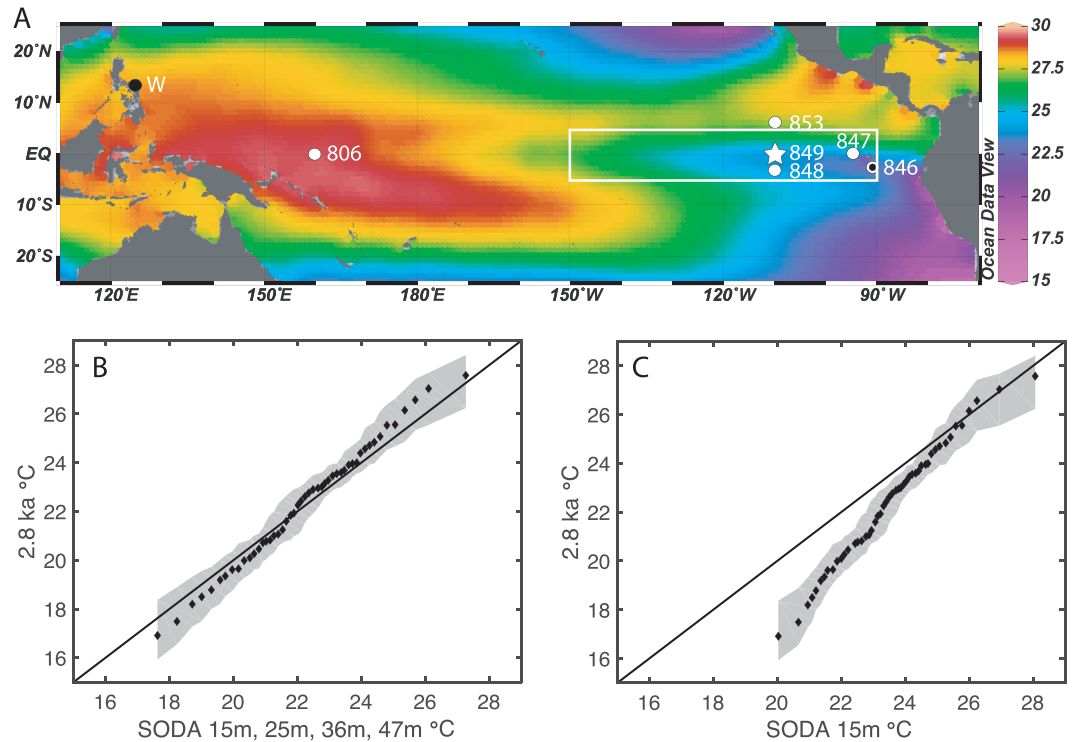


Figure 1. Sites referenced and demonstration of *G. sacculifer* as recorders of modern temperatures. (a) ODP 849 (0°N, 110°W, 3,839 m), the site of our Pliocene El Niño record (star); the sites of other Pliocene ENSO reconstructions (black circles; “W” denotes Watanabe et al., 2011, record); and Plio-Pleistocene temperature records shown in Figure 3 (white circles), superimposed on modern SST (Locarnini et al., 2013). Site 846 has both a Pliocene ENSO and a Plio-Pleistocene temperature record. White box delineates Niño3 region. (b) QQ plot of modern monthly temperatures near our site from 15, 25, 36, and 47 m depth (Carton & Giese, 2008) versus individual *G. sacculifer* temperatures from the late Holocene (2.8 ka) sample, plotted as 50 quantiles with 95% confidence intervals (gray region). Black line shows 1:1 line. Confidence intervals are estimated by bootstrapping the empirical continuous distribution function of each foraminiferal sample using Monte Carlo methods. (c) Same as (b) but with modern monthly temperatures from 15 m only.

empirical continuous distribution functions of each downcore dataset (Figure S1). See supporting information for details. As such, confidence intervals are estimated for the y axis dimension and not the x axis dimension, thus providing relative uncertainty rather than absolute uncertainty. This fits our purpose because our interpretations of dampened/similar El Niño are based on the relative comparison of Pliocene to late Holocene data. Because bootstrapping underestimates confidence intervals at the tails of a distribution, we took the additional step of performing “false positive” tests to quantify sampling uncertainty (see below, and supporting information). To identify changes in El Niño, we examine the very warmest quantiles, representative of El Niño events. A significant decrease in the temperature of the uppermost quantiles, relative to the mean, indicates a decrease in the amplitude of El Niño events compared to the late Holocene, referred to as “dampened El Niño.”

3. Results

3.1. *G. sacculifer* as Recorders of Mixed Layer Temperatures

Individual *G. sacculifer* temperatures at Site 849 from the late Holocene (dated to 2,800 years before present; Ford, Ravelo, & Polissar, 2015) provide an excellent match to the temperature distribution in the upper 50 m, in agreement with plankton tow and coretop studies (Faul et al., 2000; Ravelo et al., 1990; Watkins et al., 1996). At our site, this depth range encompasses the mixed layer and uppermost thermocline (Figures 1 and S2). Because *G. sacculifer* captures the entire temperature distribution, it appears to have little to no seasonal bias and records the full range of ENSO variability in its depth habitat. The warmest 20% of *G. sacculifer* data matches temperatures from 15 m depth (upper mixed layer), as shown by how close the points are

to the 1:1 line (Figure 1c). Because the cooler parts of the *G. sacculifer* temperature distribution come from deeper in the water column, we base our interpretations of changes in ENSO exclusively on the warmest 20% of the data, thus focusing on mixed layer temperature variability. As such, we interpret changes in El Niño amplitude and not La Niña.

To examine how changes in El Niño and seasonality at Site 849 appear in our foraminiferal data, we performed sensitivity tests. Our data can capture a decrease in El Niño amplitude of as little as 20%, and even a 50% decrease in seasonality does not affect the warmest quantiles (Figures S3 and S4). Tectonic drift in site position has a negligible effect on the temperature distribution (Figure S5). Centennial-millennial shifts in mean temperature (likely ± 0.3 to ± 0.5 °C at ODP 849; Cobb et al., 2003; Conroy et al., 2010; Rustic et al., 2015) would have little effect on our results because they have far lower amplitude than the seasonal cycle or El Niño events (White et al., 2018).

3.2. Pliocene Single Foraminiferal Temperature Data

For all our early Pliocene samples (5.038 to 3.481 Ma), the uppermost quantiles are significantly below the zero line on a normalized QQ plot, indicating dampened El Niño relative to the late Holocene sample (Figure 2). For the mid-Pliocene samples (3.071 to 3.088 Ma), some show dampened El Niño, while others show similar El Niño amplitude to the late Holocene within 95% confidence intervals. These changes in the warm tails of the Pliocene temperature distributions relative to the late Holocene can also be seen in normalized histograms (Figure S6).

To quantify sampling uncertainty (Thirumalai et al., 2013), we estimated the probability that each of our foraminiferal data sets appears to show dampened El Niño when in fact there is no change in temperature variability, that is, a “false positive” (Figure 2). These tests reflect the effects of both sample size and uncertainty in sample mean. The tests were performed by comparing 10,000 random pairs of subsamples of unaltered Simple Ocean Data Assimilation data, varying the y axis subsample sizes to exactly match those of our samples. For each subsample pair, we checked whether the average of the top four quantiles' 95% confidence intervals was as far or farther below the zero line on a normalized QQ plot, compared to each of our samples. If yes, that subsample pair was counted as a false positive (Figure S7). See supporting information for further details. For seven out of the nine samples showing dampened El Niño, the false positive rate is $\leq 5\%$. The other samples, aged 3.071 and 3.087 Ma, have much higher false positive rates but are still more likely than not to reflect dampened El Niño. Overall, the false positive tests support the idea that El Niño was generally dampened in the early Pliocene, and by the mid-Pliocene (~3.1 Ma), El Niño was sometimes dampened and sometimes similar to the late Holocene.

To test the potential effect of changes in sample mean temperature caused by shifts in thermocline depth, we constructed QQ plots normalized to the portion of the foraminiferal distribution lying entirely within the mixed layer (the warmest 50%), rather than the mean of the entire sample distribution, which spans the mixed layer and uppermost thermocline (Figure S8). We also tested the effect of Plio-Pleistocene changes in Mg/Ca of seawater, by recalculating all foraminiferal temperatures using the Evans et al. (2016) calibration (Figure S9). Additionally, we incorporated a 0.52 °C 1σ uncertainty (relative to the late Holocene data set) in every Pliocene data point (Figure S10). See supporting information for further details. In all cases, our interpretations remain the same for all samples (albeit with higher false positive rates) except the 3.071 Ma sample, which shows El Niño similar to the late Holocene.

Our data indicate that El Niño was dampened throughout the early Pliocene. By the mid-Pliocene, El Niño was sometimes weaker and sometimes stronger (similar to the late Holocene), appearing to vary on orbital timescales, though we cannot distinguish between different sources of variability. Dampened seasonality alone cannot explain our data; only dampened ENSO, or a dampening of both ENSO and seasonality, can explain our data (Figures S3 and S4).

3.3. Comparison to Existing Pliocene Proxy Data and Simulations

The record of Scroton et al. (2011) is based on individual mixed-layer and thermocline-dwelling foraminiferal $\delta^{18}\text{O}$ data from ODP Site 846, including samples from 3.076a, 3.156, 3.328, and 3.727 Ma. They concluded that ENSO persisted throughout the Pliocene but did not quantify its strength relative to today. We reanalyzed their *G. ruber* data using normalized QQ plots. Data from 3.076 and 3.328 Ma show similar El Niño to the late Holocene and data from 3.156 and 3.727 Ma show dampened El Niño (Figure S11),

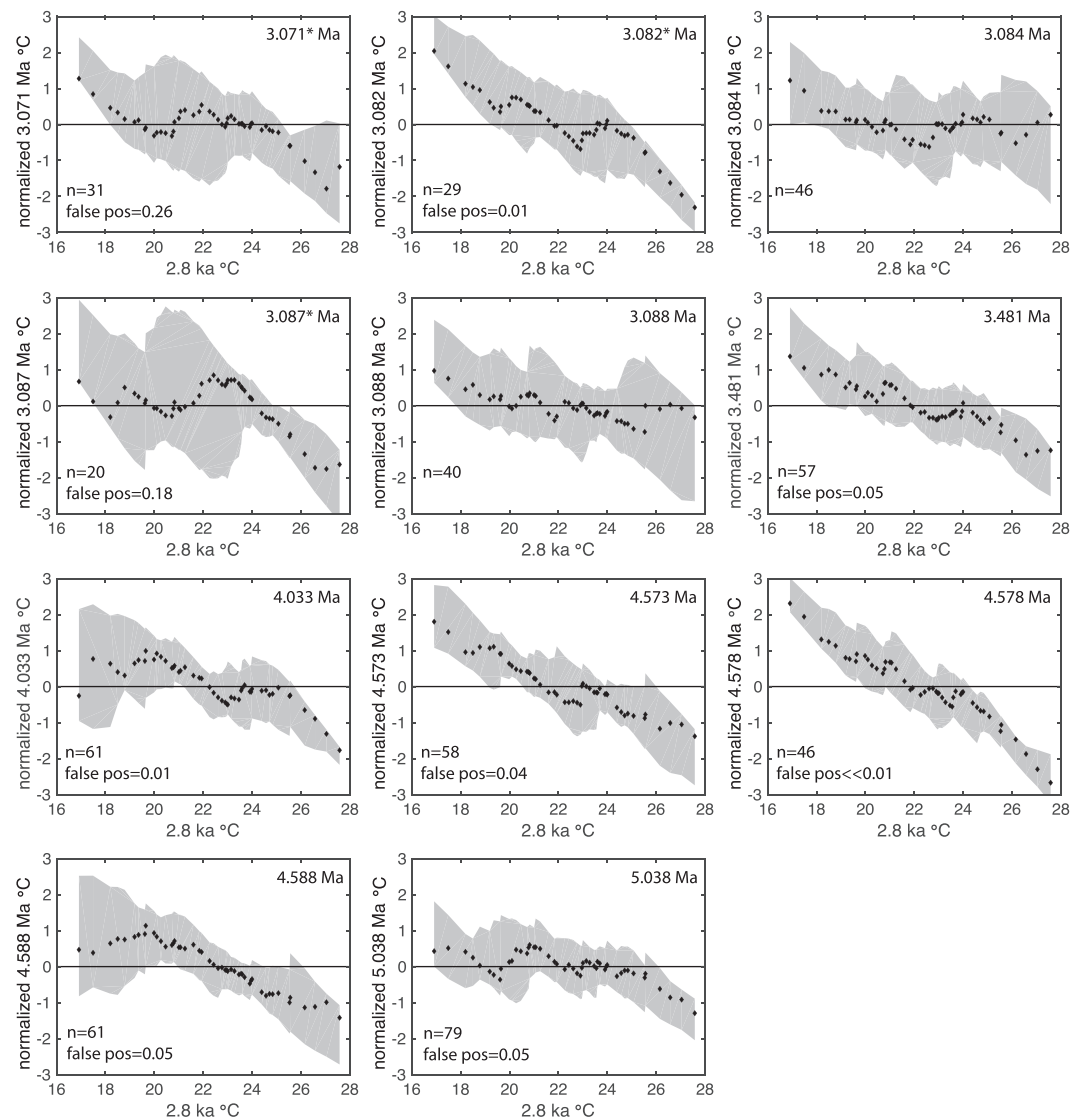


Figure 2. *G. sacculifer*-derived temperature distributions from the middle and early Pliocene at Site 849. Plots compare the late Holocene temperature distribution (x axis, all plots) to Pliocene distributions that are normalized to remove differences in mean temperature (y axis, all plots). Asterisks denote uncertainty (\pm a few thousand years) in these ages relative to all others, since they are from a different hole (849C vs. 849D). Data are plotted as 50 quantiles, and gray shading indicates 95% confidence intervals. Number of specimens and probability of that specific result being a “false positive” is indicated for each sample showing dampened El Niño.

agreeing with our findings. Watanabe et al. (2011) presented two 35-year-long coral $\delta^{18}\text{O}$ records from the Philippines from 3.5–3.8 Ma and concluded that ENSO was present but did not quantify its strength relative to today. Their data are thus consistent with ours, since we observe dampened but not necessarily absent Pliocene El Niño.

Modeling studies of Pliocene climate include (1) efforts through PlioMIP (Haywood et al., 2016) to fully recreate mid-Pliocene climate during the PRISM interval using a full suite of boundary conditions including 405 ppm $p\text{CO}_2$ and 25 m higher sea level (Dowsett et al., 2016) and (2) sensitivity tests isolating the effect on tropical Pacific mean state and ENSO of an open CAS, deeper/wider Indonesian gateway, higher $p\text{CO}_2$, weaker zonal winds and SST gradients, altered Andean orography, and a deeper thermocline; these studies are reviewed in the Discussion 4. We note that model studies report changes in ENSO, including both El Niño and La Niña, whereas we interpret changes in El Niño only.

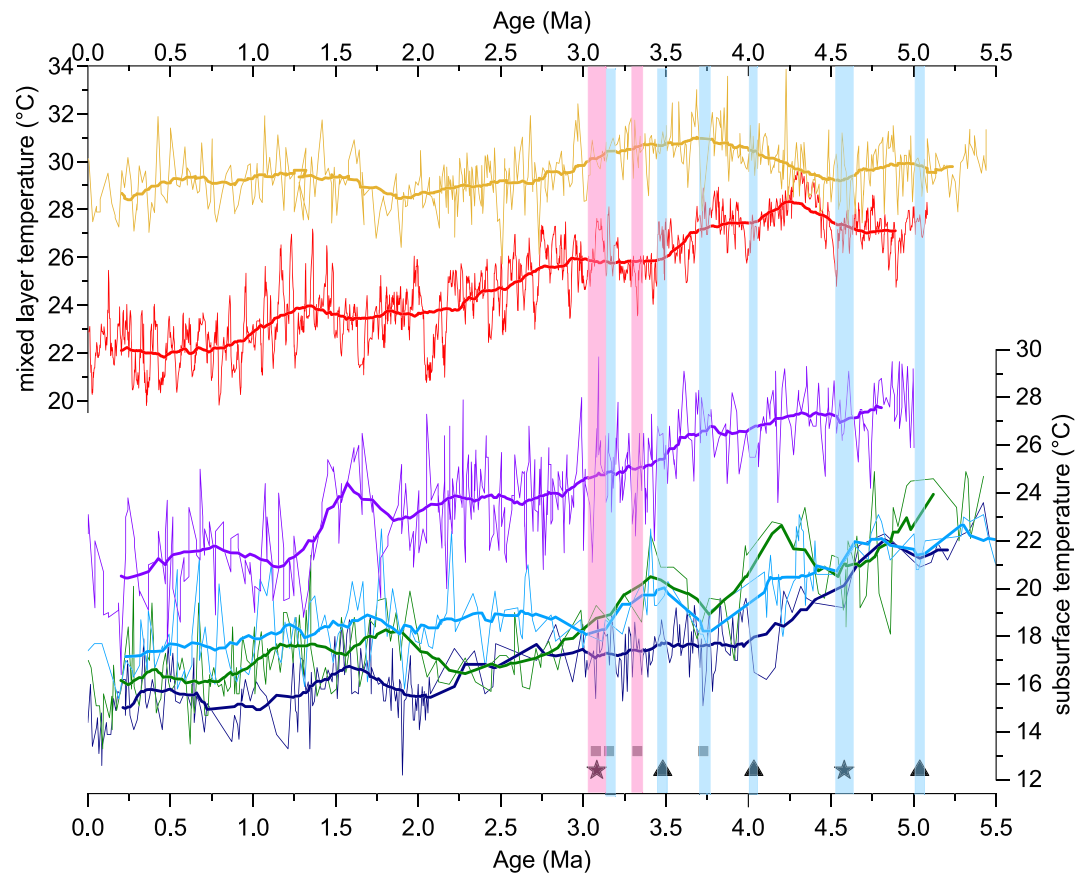


Figure 3. Plio-Pleistocene tropical Pacific temperatures and paleo-El Niño. (top) Mixed-layer temperature from *G. sacculifer* Mg/Ca at Site 806 in the west Pacific warm pool (Wara et al., 2005) and $U^{K/37}$ at Site 846 in the EEP (Lawrence et al., 2006) (red), with 400 Kyr smoothing. The 806 age model is updated, and the temperature record is adjusted for changes in Mg/Ca of seawater using the (Evans et al., 2016) calibration (Supporting Information S1). (bottom) Subsurface temperature records from *G. tumida* Mg/Ca at Site 806 (Ford, Ravelo, Dekens, et al., 2015) (purple) and Sites 853, 849, and 848 in the EEP (Ford et al., 2012) (light blue, dark blue, and green) with 400 Kyr smoothing. Symbols indicate El Niño data: Black stars and triangles (this study) denote multiple closely spaced samples and single samples; gray squares denote data from Scroxton et al. (2011). Vertical blue bars indicate dampened El Niño; red bars indicate similar El Niño as the late Holocene (or varying dampened/similar El Niño, in our multiple ~ 3.1 Ma samples); thin bars = single samples; thick bars = multiple closely spaced samples).

Eight of nine models in the PlioMIP simulated dampened ENSO (Brierley, 2015). PlioMIP models were forced with modern orbital parameters, whereas our data reflect varying orbital parameters over ~ 20 Kyr. Given the uncertainty in our sample ages (thousands of years), a direct comparison of results is not possible. Interestingly, Brierley (2015) found that neither zonal temperature gradient nor seasonal cycle nor elevation of the Andes explained results from all models—indicating that the dampening mechanism was model dependent. However, he did not explore the effect of thermocline depth.

4. Discussion

The trend in our data, with dampened El Niño throughout the early Pliocene and variable El Niño strength (sometimes dampened and sometimes similar to the late Holocene) in the mid-Pliocene, mirrors broad trends in tropical Pacific surface and subsurface temperature. Records across the tropical Pacific show a warmer subsurface in the early Pliocene, which cooled dramatically by the mid-Pliocene and continued cooling gradually toward present (Ford et al., 2012; Ford, Ravelo, Dekens, et al., 2015; Seki et al., 2012; Steph et al., 2010) (Figure 3). Vertical temperature difference (indicative of thermocline depth) was much lower than today in the early Pliocene in the EEP, approaching near-modern values around 4 Ma (Ford, Ravelo,

Dekens, et al., 2015]. Information on the evolution of EEP thermocline depth is somewhat limited by the lack of sites with both surface and subsurface temperature records spanning the Plio-Pleistocene, and the subsurface temperature record at our site is low resolution and does not contain data for each of our samples. In general, however, our observation of dampened El Niño in the early Pliocene coincides with a much deeper thermocline than today. By the mid-Pliocene, when we observe variable El Niño strength, the thermocline is inferred to have become shallow enough to interact with EEP SSTs (Lawrence et al., 2006), which may explain periods of stronger and weaker El Niño. Given the sparseness of our data between the early and mid-Pliocene, it is hard to pinpoint the timing of the transition between dampened and variable regimes.

The mechanism by which a warmer subsurface and deeper mean thermocline dampens El Niño is best understood within the framework of feedbacks (Jin et al., 2006). The thermocline takes part in the positive thermocline feedback, which helps generate ENSO. An anomalous deepening (shoaling) of the thermocline in the EEP via a decrease (increase) in east-west thermocline tilt causes warmer (cooler) SSTs in the EEP, lowering (raising) the zonal temperature gradient and weakening (strengthening) zonal winds, thus causing a further deepening (shoaling) of the EEP thermocline. Similarly, the upwelling feedback describes how an anomalous decrease (increase) in upwelling warms (cools) EEP SSTs, touching off the same chain of events and amplifying the upwelling anomaly. The strength of both feedbacks depends on a shallow mean thermocline depth in the EEP. If the mean thermocline depth is deep, then anomalies in thermocline tilt or upwelling have little impact on SSTs, which greatly weakens the strength of the feedbacks—and weak positive feedbacks cause dampened ENSO.

Manucharyan and Fedorov (2014) explored the effect of thermocline warmth/depth and zonal SST gradient on ENSO. In a fully coupled model (CESM) initialized with preindustrial conditions, they changed vertical and zonal temperature gradients by increasing/decreasing extratropical ocean mixing, in the source regions for the equatorial thermocline (which is ventilated through the shallow subtropical cells; Gu & Philander, 1997; McCreary & Lu, 1994). Increasing ocean mixing increases heat uptake and warms the equatorial thermocline, raising EEP SSTs and lowering the zonal gradient, thus allowing examination of these effects separate from other Pliocene boundary conditions (Manucharyan & Fedorov, 2014). They found that as the zonal SST gradient decreased from 5.6 °C (modern value) to 2 °C (Pliocene-like), ENSO decreased by 30–55%. Importantly for comparison to our data, the amplitude of strong El Niño events (like those shaping the warm tail of the temperature distribution) decreased even more. Similarly, Burls and Fedorov (2014) found a reduction in the amplitude of strong El Niño events in a CESM run in which cloud albedo had been altered so as to reproduce the reduced zonal and meridional SST gradients shown in Pliocene proxy data. Interestingly, this reduction in strong El Niño amplitude occurred despite little change in standard deviation of the Nino3 index (Burls & Fedorov, 2014).

From surface and subsurface temperature proxy data alone, it is not possible to determine the mechanism for dampened El Niño; as shown by Manucharyan and Fedorov (2014), the positive and negative feedbacks governing ENSO can shift in nonintuitive ways as zonal and vertical temperature gradients vary. For this reason, modeling studies are crucial for understanding mechanisms of change. Manucharyan and Fedorov (2014) show that weak (early Pliocene-like) zonal and vertical temperature gradients dampen ENSO by weakening the thermocline feedback. The zonal SST gradient may also limit El Niño SST anomalies, since the EEP cannot become warmer than the western Pacific (Burls & Fedorov, 2014). Our data verify these results, supporting the idea that vertical and zonal temperature gradients, and particularly the thermocline feedback, are important controls on ENSO strength.

The hypothesis that thermocline depth and/or warmth (i.e., vertical stratification) dictates ENSO strength has broad support in the modeling and proxy literature, beyond Manucharyan and Fedorov (2014). Liu et al. (2014) and Karamperidou et al. (2015) proposed it to explain dampened ENSO during the early and mid-Holocene. von der Heydt et al. (2011) found that weaker zonal winds weaken ENSO via the wind's effect on the strength of the thermocline feedback. Proxy studies of El Niño during the Holocene and Last Glacial Maximum also concluded that thermocline depth and/or warmth was a more important control on El Niño strength than SSTs (Ford, Ravelo, & Polissar, 2015; White et al., 2018).

Changes in oceanic gateways and Andean topography likely also affected El Niño strength, but different studies found opposing effects. A deeper/wider Indonesian seaway may have dampened (Jochum et al., 2009) or slightly strengthened ENSO (Brierley & Fedorov, 2016). An open CAS may have weakened (von der Heydt

et al., 2011) or strengthened (Song et al., 2017) ENSO or strengthened ENSO but reduced the El Niño/La Niña asymmetry such that El Niño events had a lower amplitude (Brierley & Fedorov, 2016). Lowering the Andes may strengthen ENSO (Feng & Poulsen, 2014), but full PRISM boundary conditions, which include lower Andes, weaken ENSO in the same model (Brierley, 2015). A clear disparity between studies is the exact boundary conditions imposed, for example, a CAS sill depth of 1,200 m (Song et al., 2017) versus 150 m (Brierley & Fedorov, 2016). Overall, it is difficult to use our data to validate sensitivity studies, since the timing and magnitude of gateway changes are poorly constrained. The question also remains: By what mechanism would a change in seaways or topography affect ENSO? Most proposed mechanisms act via SSTs and/or the thermocline. Our goal is to determine whether the El Padre state caused dampened El Niño, so we focus on how seaways and topography affected these parameters. Indeed, an open CAS deepens the thermocline, with deeper sill depths causing greater deepening of the thermocline (Brierley & Fedorov, 2016; Steph et al., 2010; Zhang et al., 2012). As such, we suggest that if the seaways acted on El Niño, they acted via the thermocline.

What caused sample-to-sample variations in mid-Pliocene El Niño strength? A possible explanation is precession-forced variations in thermocline warmth/depth, such that long-term and short-term changes in El Niño strength were accomplished through similar mechanisms. In the early Pliocene, the mean thermocline was likely so deep that precession-forced changes in depth could not affect the surface, rendering them incapable of affecting ENSO. By the mid-Pliocene, the mean thermocline is inferred to have shoaled enough that precession-forced changes in depth affected EEP SSTs, strengthening the thermocline feedback and enabling periods of stronger and weaker ENSO. Although records of tropical Pacific subsurface temperature (Ford et al., 2012; Ford, Ravelo, Dekens, et al., 2015) are of insufficient resolution to validate/invalidate this hypothesis for the Pliocene, it can explain dampened El Niño in the middle and early Holocene (White et al., 2018). Models show that precession can force changes in ENSO through its effect on thermocline warmth/depth and the strength of the upwelling and thermocline feedbacks (Liu et al., 2014; Lu et al., 2019). It is also possible, however, that sample-to-sample variations in mid-Pliocene El Niño strength were caused by an SST-only mechanism and/or that variations occurred on centennial (e.g., Tindall et al., 2016), not orbital, timescales.

Though our data show clear evidence for reduced amplitude of El Niño SST anomalies during the early Pliocene, the effect of those anomalies on atmospheric convection and precipitation may have been proportionally greater than today. In a climate with warmer mean EEP SSTs (including the Pliocene and projected future climate), smaller SST anomalies are required to cause the deep convection and intense precipitation in the eastern Pacific associated with “extreme El Niño” (Cai et al., 2014). As such, SST anomalies are just one part (albeit an important part) of the global impacts of ENSO.

Overall, we observe a trend in El Niño strength, with dampened El Niño throughout the early Pliocene when tropical Pacific zonal and vertical temperature gradients were much lower than today, and varying El Niño strength (sometimes dampened and sometimes similar to the late Holocene) by the mid-Pliocene, when temperature gradients were closer to modern. Our data verify the results of Manucharyan and Fedorov (2014), who found dampened ENSO when zonal and vertical temperature gradients are low, due to weakening of the thermocline feedback. The mechanism behind variations in mid-Pliocene El Niño strength is not well constrained, but precession forcing of thermocline depth is a reasonable candidate. The demonstrated importance of thermocline depth and the thermocline feedback in regulating ENSO strength should be considered in projections of ENSO’s response to anthropogenic climate change.

Acknowledgments

We thank Rob Franks for analytical assistance, Esther Brady for enlightening conversations about Pliocene ENSO, and Chris Brierley for helpful feedback on an earlier version of the manuscript. Funding was provided by NSF Grants OCE-1405178 and OCE-1204254. Data from this study are deposited at the National Oceanic and Atmospheric Administration National Climatic Data Center. The authors declare that they have no competing interests.

References

- Bijma, J., Erez, J., & Hemleben, C. (1990). Lunar and semi-lunar reproductive cycles in some spinose planktonic foraminifera. *Journal of Foraminiferal Research*, 20(2), 117–127. <https://doi.org/10.2113/gsjfr.20.2.117>
- Brierley, C. M. (2015). Interannual climate variability seen in the Pliocene Model Intercomparison Project. *Climate of the Past*, 11(3), 605–618. <https://doi.org/10.5194/cp-11-605-2015>
- Brierley, C. M., & Fedorov, A. V. (2016). Comparing the impacts of Miocene–Pliocene changes in inter-ocean gateways on climate: Central American Seaway, Bering Strait, and Indonesia. *Earth and Planetary Science Letters*, 444, 116–130. <https://doi.org/10.1016/j.epsl.2016.03.010>
- Burls, N. J., & Fedorov, A. V. (2014). Simulating Pliocene warmth and a permanent El Niño-like state: The role of cloud albedo. *Paleoceanography*, 29, 893–910. <https://doi.org/10.1002/2014pa002644>
- Cai, W., Borlace, S., Lengaigne, M., van Rensch, P., Collins, M., Vecchi, G., et al. (2014). Increasing frequency of extreme El Niño events due to greenhouse warming. *Nature Climate Change*, 4(2), 111–116. <https://doi.org/10.1038/nclimate2100>

- Carton, J. A., & Giese, B. S. (2008). A reanalysis of ocean climate using Simple Ocean Data Assimilation (SODA). *Monthly Weather Review*, 136(8), 2999–3017. <https://doi.org/10.1175/2007mwr1978.1>
- Chen, L., Li, T., Yu, Y., & Behera, S. K. (2017). A possible explanation for the divergent projection of ENSO amplitude change under global warming. *Climate Dynamics*, 49(11–12), 3799–3811. <https://doi.org/10.1007/s00382-017-3544-x>
- Cobb, K. M., Charles, C. D., Cheng, H., & Edwards, R. L. (2003). El Niño–Southern Oscillation and tropical Pacific climate during the last millennium. *Nature*, 424(6946), 271–276. <https://doi.org/10.1038/nature01779>
- Conroy, J. L., Overpeck, J. T., & Cole, J. E. (2010). El Niño/Southern Oscillation and changes in the zonal gradient of tropical Pacific sea surfacetemperature over the last 1.2 ka. *PAGES News*, 18(1), 32–34.
- Dekens, P. S., Lea, D. W., Pak, D. K., & Spero, H. J. (2002). Core top calibration of Mg/Ca in tropical foraminifera: Refining paleotemperature estimation. *Geochemistry, Geophysics, Geosystems*, 3(4), 1022. <https://doi.org/10.1029/2001GC000200>
- Dekens, P. S., Ravelo, A. C., & McCarthy, M. D. (2007). Warm upwelling regions in the Pliocene warm period. *Paleoceanography*, 22, PA3211. <https://doi.org/10.1029/2006pa001394>
- Dowsett, H., Dolan, A., Rowley, D., Moucha, R., Forte, A. M., Mitrovica, J. X., et al. (2016). The PRISM4 (mid-Piacenzian) paleoenvironmental reconstruction. *Climate of the Past*, 12(7), 1519–1538. <https://doi.org/10.5194/cp-12-1519-2016>
- Evans, D., Brierley, C., Raymo, M. E., Erez, J., & Müller, W. (2016). Planktic foraminifera shell chemistry response to seawater chemistry: Pliocene–Pleistocene seawater Mg/Ca, temperature and sea level change. *Earth and Planetary Science Letters*, 438, 139–148. <https://doi.org/10.1016/j.epsl.2016.01.013>
- Faul, K. L., Ravelo, A. C., & Delaney, M. L. (2000). Reconstructions of upwelling, productivity, and photic zone depth in the eastern equatorial Pacific Ocean using planktonic foraminiferal stable isotopes and abundances. *Journal of Foraminiferal Research*, 30(2), 110–125. <https://doi.org/10.2113/0300110>
- Feng, R., & Poulsen, C. J. (2014). Andean elevation control on tropical Pacific climate and ENSO. *Paleoceanography*, 29, 795–809. <https://doi.org/10.1002/2014pa002640>
- Ford, H. L., Ravelo, A. C., Dekens, P. S., LaRiviere, J. P., & Wara, M. W. (2015). The evolution of the equatorial thermocline and the early Pliocene El Padre mean state. *Geophysical Research Letters*, 42, 4878–4887. <https://doi.org/10.1002/>
- Ford, H. L., Ravelo, A. C., & Hovan, S. (2012). A deep Eastern Equatorial Pacific thermocline during the early Pliocene warm period. *Earth and Planetary Science Letters*, 355–356, 152–161. <https://doi.org/10.1016/j.epsl.2012.08.027>
- Ford, H. L., Ravelo, A. C., & Polissar, P. J. (2015). Reduced El Niño–Southern Oscillation during the Last Glacial Maximum. *Science*, 347(6219), 255–258. <https://doi.org/10.1126/science.1258437>
- Gu, D., & Philander, S. G. H. (1997). Interdecadal climate fluctuations that depend on exchanges between the tropics and extratropics. *Science*, 275(5301), 805–807. <https://doi.org/10.1126/science.275.5301.805>
- Haywood, A. M., Dowsett, H. J., Dolan, A. M., Rowley, D., Abe-Ouchi, A., Otto-Bliesner, B., et al. (2016). The Pliocene Model Intercomparison Project (PlioMIP) Phase 2: Scientific objectives and experimental design. *Climate of the Past*, 12(3), 663–675. <https://doi.org/10.5194/cp-12-663-2016>
- Jin, F.-F., Kim, S. T., & Bejarano, L. (2006). A coupled-stability index for ENSO. *Geophysical Research Letters*, 33, L23708. <https://doi.org/10.1029/2006gl027221>
- Jochum, M., Fox-Kemper, B., Molnar, P. H., & Shields, C. (2009). Differences in the Indonesian seaway in a coupled climate model and their relevance to Pliocene climate and El Niño. *Paleoceanography*, 24, PA1212. <https://doi.org/10.1029/2008pa001678>
- Karamperidou, C., Di Nezio, P. N., Timmermann, A., Jin, F.-F., & Cobb, K. M. (2015). The response of ENSO flavors to mid-Holocene climate: Implications for proxy interpretation. *Paleoceanography*, 30, 527–547. <https://doi.org/10.1002/2014pa002742>
- Kim, S. T., Cai, W., Jin, F.-F., & Yu, J.-Y. (2014). ENSO stability in coupled climate models and its association with mean state. *Climate Dynamics*, 42(11–12), 3313–3321. <https://doi.org/10.1007/s00382-013-1833-6>
- Lawrence, K. T., Liu, Z., & Herbert, T. D. (2006). Evolution of the eastern tropical Pacific through Plio-Pleistocene glaciation. *Science*, 312(5770), 79–83. <https://doi.org/10.1126/science.1120395>
- Liu, Z., Lu, Z., Wen, X., Otto-Bliesner, B. L., Timmermann, A., & Cobb, K. M. (2014). Evolution and forcing mechanisms of El Niño over the past 21,000 years. *Nature*, 515(7528), 550–553. <https://doi.org/10.1038/nature13963>
- Locarnini, R. A., Mishonov, A. V., Antonov, J. I., Boyer, T. P., Garcia, H. E., Baranova, O. K., et al. (2013). In S. Levitus (Ed.), *World Ocean Atlas 2013, Volume 1: Temperature*, NOAA Atlas NESDIS, (Vol. 73, p. 40). Washington, DC: U.S. Government Printing Office.
- Lu, Z., Liu, Z., Chen, G., & Guan, J. (2019). Prominent precession band Variance in ENSO intensity over the last 300,000 years. *Geophysical Research Letters*, 46, 9786–9795. <https://doi.org/10.1029/2019gl083410>
- Manucharyan, G. E., & Fedorov, A. V. (2014). Robust ENSO across a wide range of climates. *Journal of Climate*, 27(15), 5836–5850. <https://doi.org/10.1175/jcli-d-13-00759.1>
- McCreary, J. P., & Lu, P. (1994). Interaction between the subtropical and equatorial ocean circulations: the subtropical cell. *Journal of Physical Oceanography*, 24, 466–497.
- Mix, A. C., Pisias, N. G., Rugh, W., Wilson, J., Morey, A., & Hagelberg, T. K. (1995). Benthic foraminifer stable isotope record from site 849 (0–5 Ma): Local and global climate changes. In N. G. Pisias, L. A. Mayer, T. R. Janecek, A. Palmer-Julson, & T. H. van Andel (Eds.), *Proceedings of the Ocean Drilling Program, Scientific Results* (pp. 371–412). College Station TX: Ocean Drilling Program.
- Ravelo, A. C., Fairbanks, R. G., & Philander, S. G. H. (1990). Reconstructing tropical Atlantic hydrography using planktonic foraminifera and an ocean model. *Paleoceanography*, 5(3), 409–431. <https://doi.org/10.1029/PA005i003p00409>
- Rousselle, G., Beltran, C., Sicre, M.-A., Raffi, I., & De Rafélis, M. (2013). Changes in sea-surface conditions in the Equatorial Pacific during the middle Miocene–Pliocene as inferred from coccolith geochemistry. *Earth and Planetary Science Letters*, 361, 412–421. <https://doi.org/10.1016/j.epsl.2012.11.003>
- Rustic, G. T., Koutavas, A., Marchitto, T. M., & Linsley, B. K. (2015). Dynamical excitation of the tropical Pacific Ocean and ENSO variability by Little Ice Age cooling. *Science*, 350(6267), 1537–1541. <https://doi.org/10.1126/science.aac9937>
- Scroton, N., Bonham, S. G., Rickaby, R. E. M., Lawrence, S. H. F., Hermoso, M., & Haywood, A. M. (2011). Persistent El Niño–Southern Oscillation variation during the Pliocene Epoch. *Paleoceanography*, 26, PA2215. <https://doi.org/10.1029/2010pa002097>
- Seki, O., Schmidt, D. N., Schouten, S., Hopmans, E. C., Sinninghe Damsté, J. S., & Pancost, R. D. (2012). Paleoceanographic changes in the Eastern Equatorial Pacific over the last 10 Myr. *Paleoceanography*, 27, PA3224. <https://doi.org/10.1029/2011pa002158>
- Song, Z., Latif, M., Park, W., Krebs-Kanzow, U., & Schneider, B. (2017). Influence of seaway changes during the Pliocene on tropical Pacific climate in the Kiel climate model: Mean state, annual cycle, ENSO, and their interactions. *Climate Dynamics*, 48(11–12), 3725–3740. <https://doi.org/10.1007/s00382-016-3298-x>

- Spezzaferri, S., Kucera, M., Pearson, P. N., Wade, B. S., Rappo, S., Poole, C. R., et al. (2015). Fossil and genetic evidence for the polyphyletic nature of the planktonic foraminifera "Globigerinoides," and description of the new genus *Trilobatus*. *PLoS One*, *10*, e0128108. <https://doi.org/10.1371/journal.pone.0128108>
- Steph, S., Tiedemann, R., Prange, M., Groeneveld, J., Schulz, M., Timmermann, A., et al. (2010). Early Pliocene increase in thermohaline overturning: A precondition for the development of the modern equatorial Pacific cold tongue. *Paleoceanography*, *25*, PA2202. <https://doi.org/10.1029/2008pa001645>
- Thirumalai, K., Partin, J. W., Jackson, C. S., & Quinn, T. M. (2013). Statistical constraints on El Niño Southern Oscillation reconstructions using individual foraminifera: A sensitivity analysis. *Paleoceanography*, *28*, 401–412. <https://doi.org/10.1002/palo.20037>
- Tindall, J. C., Haywood, A. M., & Howell, F. W. (2016). Accounting for centennial-scale variability when detecting changes in ENSO: A study of the Pliocene. *Paleoceanography*, *31*, 1330–1349. <https://doi.org/10.1002/2016pa002951>
- Trauth, M. H., Sarnthein, M., & Arnold, M. (1997). Bioturbational mixing depth and carbon flux at the seafloor. *Paleoceanography*, *12*(3), 517–526. <https://doi.org/10.1029/97PA00722>
- von der Heydt, A. S., Nnaffe, A., & Dijkstra, H. A. (2011). Cold tongue/Warm pool and ENSO dynamics in the Pliocene. *Climate of the Past*, *7*(3), 903–915. <https://doi.org/10.5194/cp-7-903-2011>
- Wara, M. W., Ravelo, A. C., & Delaney, M. L. (2005). Permanent El Niño-like conditions during the Pliocene Warm Period. *Science*, *309*(5735), 758–761. <https://doi.org/10.1126/science.1112596>
- Watanabe, T., Suzuki, A., Minobe, S., Kawashima, T., Kameo, K., Minoshima, K., et al. (2011). Permanent El Niño during the Pliocene warm period not supported by coral evidence. *Nature*, *471*(7337), 209–211. <https://doi.org/10.1038/nature09777>
- Watkins, J. M., Mix, A. C., & Wilson, J. (1996). Living planktic foraminifera: Tracers of circulation and productivity regimes in the central equatorial Pacific. *Deep Sea Research Part II: Topical Studies in Oceanography*, *43*(4-6), 1257–1282. [https://doi.org/10.1016/0967-0645\(96\)00008-2](https://doi.org/10.1016/0967-0645(96)00008-2)
- White, S. M., Ravelo, A. C., & Polissar, P. J. (2018). Dampened El Niño in the early and mid-Holocene due to insolation-forced warming/deepening of the thermocline. *Geophysical Research Letters*, *45*, 316–326. <https://doi.org/10.1002/2017GL075433>
- Zhang, X., Prange, M., Steph, S., Butzin, M., Krebs, U., Lunt, D. J., et al. (2012). Changes in equatorial Pacific thermocline depth in response to Panamanian seaway closure: Insights from a multi-model study. *Earth and Planetary Science Letters*, *317*–*318*, 76–84. <https://doi.org/10.1016/j.epsl.2011.11.028>
- Zhang, Y. G., Pagani, M., & Liu, Z. (2014). A 12-million-year temperature history of the tropical Pacific Ocean. *Science*, *344*(6179), 84–87. <https://doi.org/10.1126/science.1246172>